CHEMISTRY
A EUROPEAN JOURNAL

FULL PAPER

DOI: 10.1002/chem.201302020

Conformational Change from a Twisted Figure-Eight to an Open-Extended Structure in Doubly Fused 36π Core-Modified Octaphyrins Triggered by Protonation: Implication on Photodynamics and Aromaticity

Ganesan Karthik,[a] Jong Min Lim,[b] A. Srinivasan,[a] C. H. Suresh,[c] Dongho Kim,*[b] and Tavarekere K. Chandrashekar*[a]

Dedicated to Dr. T. Ramasami on the occasion of his 65th birthday

Abstract: Two examples of core-modified 36π doubly fused octaphyrins that undergo a conformational change from a twisted figure-eight to an open-extended structure induced by protonation are reported. Syntheses of the two octaphyrins (in which Ar = mesityl or tolyl) were achieved by a simple acid-catalyzed condensation of dipyrrane unit containing an electron-rich, rigid dithienothiophene (DTT) core with pentafluorobenzaldehyde followed by oxidation with 2,3-dichloro-5,6-dicyano-1,4-benzoquinone (DDQ). The single-crystal X-ray structure of the octaphyrin (in which Ar = mesityl) shows a figure-eight twisted conformation of the expanded porphyrin skeleton with two DTT moieties oriented in a staggered conformation with a π-cloud distance of 3.7 Å. Spectroscopic and quantum mechanical calculations reveal that both octaphyrins conform to a [4n]π nonaromatic electronic structure. Protonation of the pyrrole nitrogen atoms of the octaphyrins results in dramatic structural change, which led to 1) a large redshift and sharpening of absorption bands in electronic absorption spectrum, 2) a large change in chemical shift of pyrrole β-CH and −NH protons in the ^{1}H NMR spectrum, 3) a small increase in singlet lifetimes, and 4) a moderate increase in two-photon absorption cross-section values. Furthermore, nucleus-independent chemical shift (NICS) values calculated at various geometrical positions show positive values and anisotropy-induced current density (AICD) plots indicate paratropic ring-currents for the diprotonated form of the octaphyrin (in which Ar = tolyl); the single-crystal X-ray structure of the diprotonated form of the octaphyrin shows an extended structure in which one of the pyrrole ring of each dipyrrin subunit undergoes a 180° ring-flip. Four trifluoroacetic acid (TFA) molecules are bound above and below the molecular plane defined by *meso*-carbon atoms and are held by N−H···O, N−H···F, and C−H···F intermolecular hydrogen-bonding interactions. The extended-open structure upon protonation allows π-delocalization and the electronic structure conforms to a [4n]π Hückel antiaromatic in the diprotonated state.

Keywords: aromaticity · conformation analysis · fused-ring systems · photodynamics · X-ray diffraction

Introduction

Expanded porphyrins continue to attract the attention of researchers because of their diverse applications as new-generation nonlinear optical (NLO) materials,[1] photosensitizers for photodynamic therapy (PDT),[2] cation and anion receptors,[3] magnetic resonance imaging (MRI) contrasting agents,[4] and to address fundamental properties of aromaticity in larger cyclic π-systems.[5] The reasons for their involvement in such diverse applications are their rich structural diversity.[6] Expanded porphyrins exhibit normal,[7] inverted,[8] fused,[9] confused,[10] figure-eight,[11] Möbius,[12] and bridged[13] conformations depending on the number and nature of the heterocyclic rings and the way these rings are connected to each other through *meso*-carbon bridges. Furthermore, it is possible to convert one into another by simple chemical stimuli such as protonation,[14] change of solvent and temperature,[15] ring fusion,[9] metal coordination,[16] and so on. For example, recently it has been shown that di-*p*-benzi[28]hexaphyrin **1** can act as a Hückel–Möbius

[a] G. Karthik, Dr. A. Srinivasan, Prof. Dr. T. K. Chandrashekar
School of Chemical Sciences, National Institute of Science Education and Research (NISER), IOP Campus, Bhubaneshwar 751005, Odisha (India)
E-mail: tkc@niser.ac.in

[b] Dr. J. M. Lim, Prof. Dr. D. Kim
Department of Chemistry, Yonsei University
Shinchon-dong 134, Seodaemoon-gu
Seoul 120-749 (Korea)
E-mail: dongho@yonsei.ac.kr

[c] Dr. C. H. Suresh
Inorganic Chemistry Section
Chemical Sciences and Technology Division
National Institute for Interdisciplinary Science and Technology (CSIR), Thiruvananthapuram 695019, Kerala (India)

Supporting information for this article is available on the WWW under http://dx.doi.org/10.1002/chem.201302020.

topology switch upon changing the solvent from nonpolar to polar and a change of temperature.[17] Hexaphyrins, a class of expanded porphyrins are conformationally flexible and depending upon the solvent of crystallization both Möbius aromatic and Hückel antiaromatic systems have been isolated in 28π hexaphyrin systems **2**.[18] The 24π fused-expanded porphyrin **3**, which exhibits a Hückel antiaromatic conformation, can be converted into Möbius aromatic conformation by Rh^I coordination.[19] Chandrashekar and co-workers have reported that the Rh^I coordination in a oxasmaragdyrin cavity increases the two-photon absorption (TPA) cross-section values by more than ten times, which has been attributed to restoration of π-electron conjugation upon Rh^I coordination.[1e] More recently, it has been shown that in 26π hexaphyrin **4**, upon introduction of a thiophene bridge between two opposite *meso*-carbon atoms, changes the electronic delocalization pathway where the bridging thiophene group takes part in electron conjugation of the macrocycle.[13a] Such changes in the electron conjugation pathway leads to an increase in TPA cross-section values relative to its nonbridged congener. Thus, it is important to study such subtle structural changes in expanded porphyrin systems upon simple chemical stimulation to design molecules for a specific application.

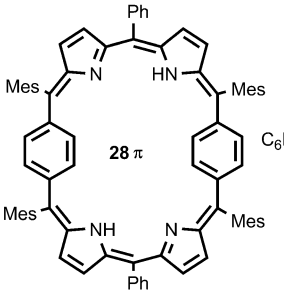

1

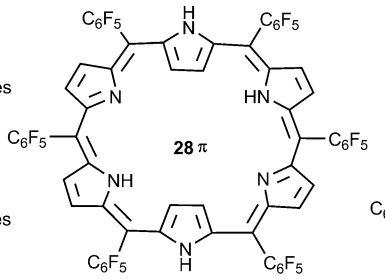

2

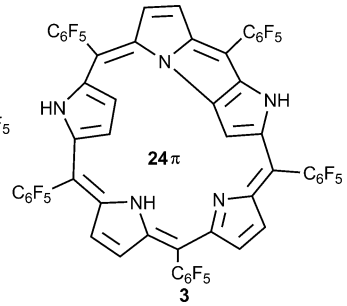

3

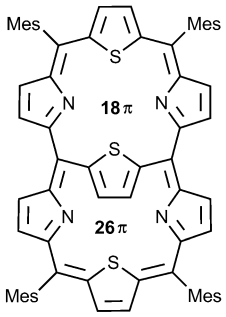

4

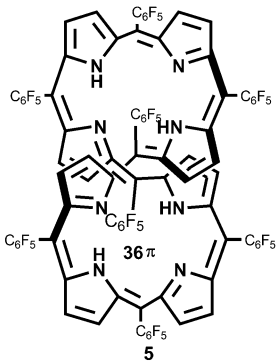

5

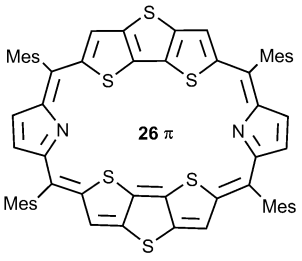

6

Protonation of pyrrole nitrogen atoms has been often used to interconvert one structure into another. For example Latos-Grażyński and co-workers have shown that it is possible to convert an inverted structure into a normal structure by protonation in sapphyrins.[8a,b] Osuka and co-workers have shown that the structure of rubyrins depends on the nature of the acid used for protonation.[8c] The use of HCl leads to a normal rubyrin structure, whereas the use of TFA results in an inverted rubyrin structure in which two pyrrole rings show a 180° flip. More recently, Osuka, Kim, and co-workers have used protonation to study conformational changes from Hückel antiaromatic and nonaromatic systems to aromatic Möbius conformation in 32π heptaphyrins[14] and 36π octaphyrins,[20] respectively. Specifically, 32π heptaphyrins, which exhibit Hückel antiaromatic conformation, changes its conformation to a Möbius aromatic one upon protonation by TFA. On the other hand, the 36π octaphyrin with a twisted figure-eight conformation in the free-base form, changes into an open-extended structure upon protonation. The driving force for such a structural change is attributed to the breaking of intramolecular hydrogen bonds in the free-base form and formation of intermolecular hydrogen bonds with TFA in the dicationic form. Detailed photophysical studies revealed an increase in excited singlet- and triplet-state lifetimes, which are attributable to the rigidity of the macrocycle in the dicationic form. The TPA values increases more than four times in the dicationic form and this has been explained in terms of attaining Möbius aromatic character of the macrocycle in the extended structure.

In this article, we wish to report the two examples of core-modified doubly fused 36π octaphyrins **7** and **8**, which exhibit a dramatic change from a twisted figure-eight conformation in the free-base form to an open-extended conformation upon protonation. However, unlike the 36π octaphyrins reported by Osuka, Kim, and co-workers, this structural change does not accompany changes of Hückel–Möbius aromaticity switching.[20] Thus, fused octaphyrins, which are nonaromatic in the free-base form, change to a [4n]π Hückel antiaromatic in the diprotonated state due to an open-extended structure. Spectroscopic and theoretical studies on the free-base and diprotonated forms support the presence of paratropic ring-current and positive NICS values justifying such a conclusion. The excited-state photodynamics reveal a small increase in excited singlet-state lifetime in the mono- and diprotonated state and the TPA values also show a moderate increase in the protonated derivatives, presumably due to the open structure and the local aromaticity of the fused-dithienothiophene (DTT) moieties.

Results and Discussion

Synthesis: Expanded porphyrins, by virtue of their rich structural diversity,[6] are well-suited for the creation of Möbius/Hückel switching and several reports have already appeared in the literature that exhibit such changes in topology under various physical or chemical stimuli.[12,14,20] Our synthetic strategy involved incorporation of half-rigid and half-flexible subunits in an expanded porphyrin skeleton with appropriate linking groups. The rigid precursor we have chosen was DTT, which has an electron-rich core.[9b,21] The key precursors, fused DTT-diol (**9** or **10**) was treated with pyrrole in presence of 0.2 equivalents of trifluoroacetic acid to obtain the fused DTT-dipyrrane (**11** or **12**) in 85% yield (Scheme 1). A further acid-catalyzed condensation of **11** or **12** with an equal amount of pentafluorobenzaldehyde in presence of 0.3 equivalents of *p*-toluenesulfonic acid followed by oxidation with 2,3-dichloro-5,6-dicyano-1,4-benzoquinone (DDQ) gave the crude product. Repeated purification by column chromatography over basic alumina followed by silica gel (100–200 mesh) with CH_2Cl_2/hexane (30:70) gave a pink fraction, which was identified as the doubly fused octaphyrins **7** or **8**. After evaporation of the solvent, a green-colored solid was isolated in 7–10% yield. The composition of **7** and **8** were confirmed by mass spectral analysis. Octaphyrin **7** shows the parent ion peak at *m/z* 1417.1589 [$M+H^+$], whereas **8** was found at 1529.287 [$M+H^+$] (see the Supporting Information).

In cyclic voltammetry, octaphyrin **7** shows two reversible oxidation peaks (+1.11, +1.25 V) and two reversible reduction peaks (+0.421, +0.204 V) against the $Ag/AgNO_3$ reference electrode in dichloromethane (see the Supporting Information). This voltammetric behavior encouraged us to try chemical oxidation and reduction of **7**. Oxidation with MnO_2 in dichloromethane resulted in the ring opening of the macrocycle giving two products with *m/z* 741.2 and 1049.8 (see the Supporting Information). Chemical reduction with $NaBH_4$ results in decomposition of the macrocycle.

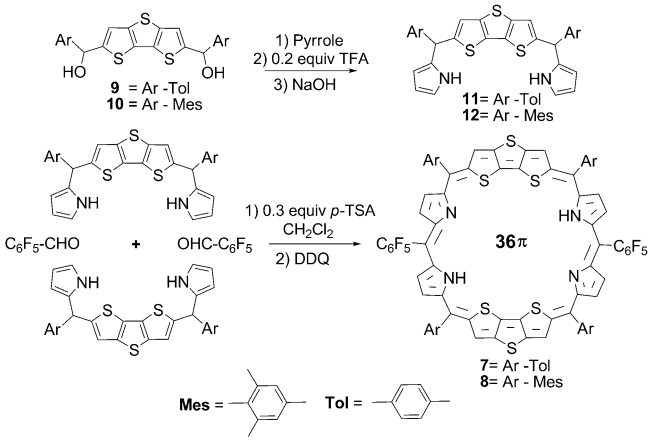

Scheme 1. Syntheses of doubly fused octaphyrins.

^{1}H NMR characterization: The ^{1}H NMR spectra of **7** and its diprotonated derivative **7**·2H$^+$ along with the assignments are shown in Figure 1. The two inner-NH protons of pyrrole ring in **7** resonate as a singlet in the deshielded region at $\delta =$

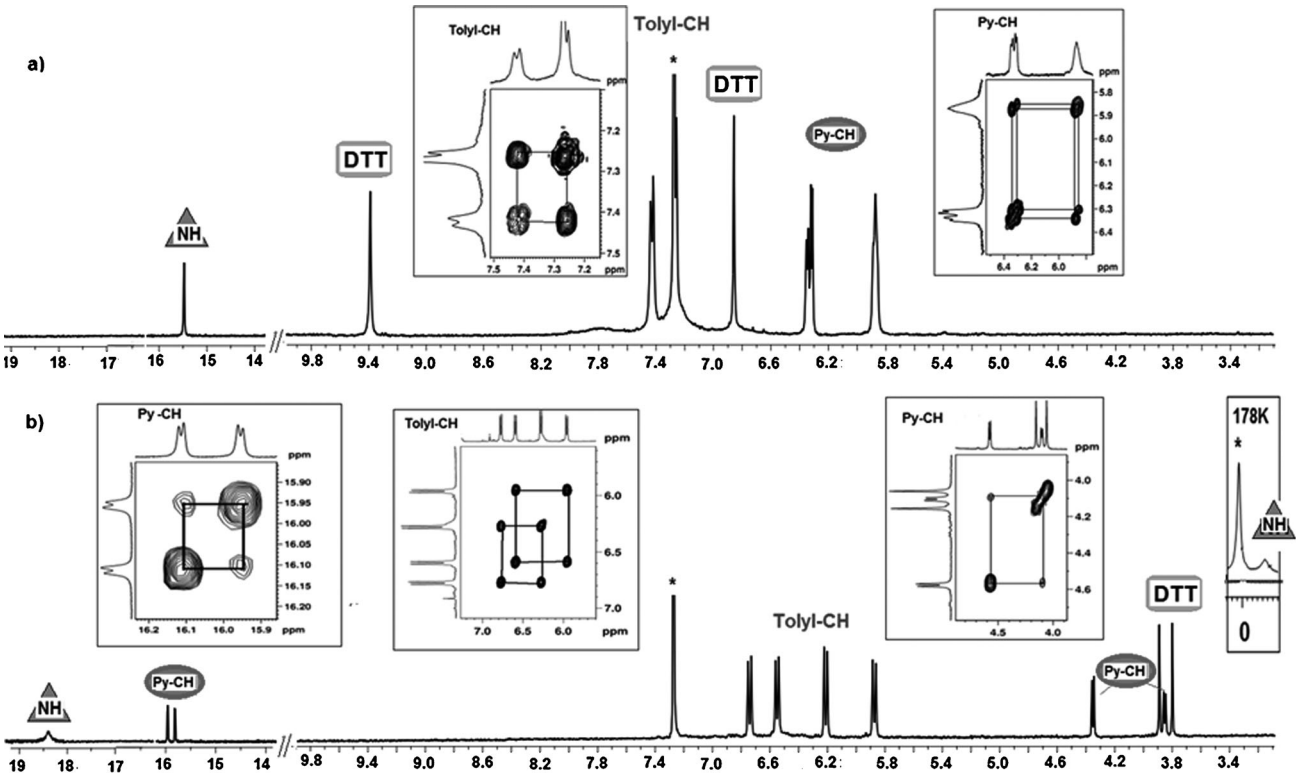

Figure 1. ^{1}H NMR spectra of **7** in $CDCl_3$ (1 mM): a) before and b) after protonation by TFA; inset: ^{1}H–^{1}H COSY correlations.

15.48 ppm and this assignment was confirmed by using a D_2O-exchange experiment. Two multiplets centered at $\delta =$ 6.32 and 5.87 ppm are assigned to four pyrrole β-CH protons and this assignment was confirmed by using a ^1H–^1H correlation spectroscopy (COSY) experiment (Figure 1, inset).

The *meso*-tolyl-CH protons appear as a doublet of doublet at $\delta = 7.25$ and 7.41 ppm (confirmed by ^1H–^1H COSY spectrum, Figure 1, inset). Four DTT ring protons appear as two sharp singlets at $\delta = 9.38$ and 6.85 ppm and the NOESY experiment confirms the presence of long-range correlation between these protons. *meso*-Tolyl-CH_3 protons resonate as two singlets at $\delta = 2.48$ and 2.45 ppm (see the Supporting Information). Furthermore, the ^1H NMR spectrum of **7** did not show any major changes in the chemical shift on varying the temperature from 298–178 K, except that the resolution of the spectrum was better at 178 K (see the Supporting Information). This observation suggests that there is no change in the structure of the macrocycle upon temperature variation. However, at 343 K the spectrum became broad. The ^1H NMR data, on comparison with the data reported for other expanded porphyrins suggest that **7** in its free-base form conforms to the 36π twisted figure-eight structure and is nonaromatic.[14,20]

Major changes were observed in ^1H NMR spectrum on protonation of **7** by TFA in $CDCl_3$ solution at 298 K. The changes are: 1) two broad NH signals were observed at $\delta =$ 18.7 and −0.1 ppm (the peak at $\delta = -0.1$ ppm was observed only at 178 K); 2) two sets of pyrrole β-CH resonances; a doublet of doublet centered at $\delta = 15.91$ ppm ($^3J = 5.2$ Hz) and other at $\delta = 4.36$ ppm ($^3J = 5.2$ Hz; assignment confirmed by ^1H–^1H COSY spectrum, inset in Figure 1); 3) the tolyl-CH protons are shielded and appear as four doublets in the region $\delta = 5.97$–6.78 ppm and 4) the DTT protons are shielded relative to free-base form and appear as two sharp singlets at $\delta = 4.17$ and 4.08 ppm. These results suggest a major structural change upon protonation.

The appearance of two sets of pyrrolic β-CH protons in the shielded and deshielded region is attributed to ring inversions in which one pyrrole ring of each dipyrrin subunits undergoes an 180° rotation, which are common in core-modified expanded porphyrins (Scheme 2).[6] This interpretation also accounts for observation of two separate NH signals in the shielded and deshielded region. Pyrrole-ring inversion upon protonation of **7** led us to have two possible ways of interpretation of the ring-current effect (paratropic vs. diatropic) in the macrocycle.

If the protonated derivatives are aromatic ([4n]π Möbius), one would expect a large diatropic ring-current, which is reflected in the chemical shifts of β-CH and −NH protons for normal and inverted pyrrole rings. In such a scenario, the following assignment holds: normal pyrrole ring: (β-CH: $\delta = 15.91$ and −NH: −0.1 ppm); inverted pyrrole ring: (β-CH: $\delta = 4.36$ and −NH: 18.7 ppm). Hence, the corresponding $\Delta\delta$ values are 16.1 and 14.34 ppm for normal and inverted pyrrole rings, respectively.

If the protonated derivatives are antiaromatic ([4n]π Hückel), one would expect a large paratropic ring-current. In such a case, the following assignment holds: Normal pyrrole ring: (β-CH: $\delta = 4.36$ and −NH: 18.7 ppm); inverted pyrrole ring: (β-CH: $\delta = 15.91$ and −NH: −0.1 ppm).

However, other spectroscopic data and theoretical calculations support the later assignment. Thus, octaphyrin **7** exhibits the antiaromatic character with extension of π-conjugation upon protonation. The observed upfield shift of DTT protons upon protonation also supports such a conclusion.

Structural characterization: The explicit structure of **8** was unambiguously confirmed by single-crystal X-ray diffraction analysis, in which the macrocycle crystallizes in a monoclinic system with *P*21/*n* space group (Figure 2). As predicted from the NMR spectral analysis, the structure adopts figure-eight conformation in the solid state with 36π-electron circuit. There are two dipyrrin moieties and two DTT units that are connected through the six *meso*-carbon bridges by mesityl and pentafluorophenyl units, in which all the pyrrolic nitrogen atoms point inwards. The amino (N2-H2A and N3-H3) and imino (N1 and N4) nitrogen atoms that are in the dipyrrin moieties are in strong intramolecular hydrogen-bonding interactions (N2-H2A···N1 and N3-H3···N4) with distances of 2.13 and 2.20 Å and angles of 124°, respectively. Both the DTT moieties are staggered and appended one over the other with the π-cloud distance of 3.70 Å. This ob-

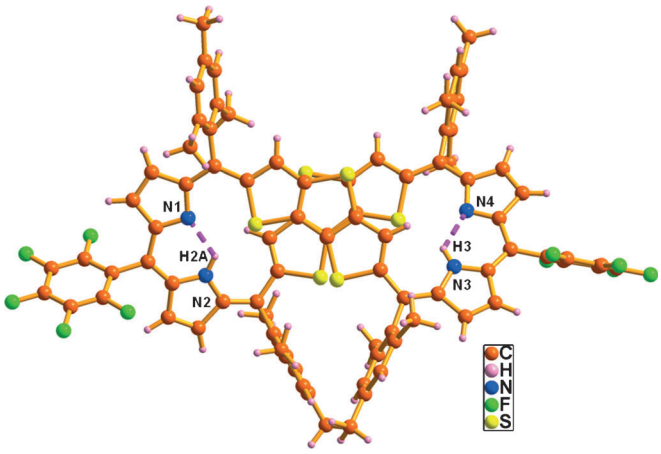

Figure 2. Single-crystal X-ray structure of **8**.

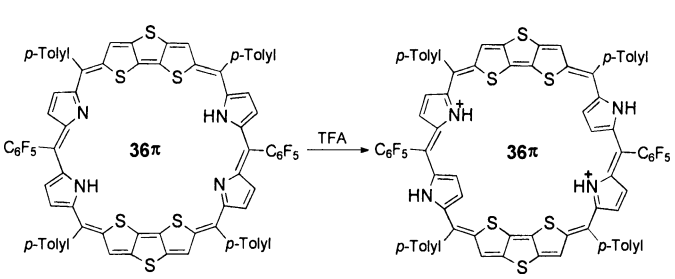

Scheme 2. Ring-inversion of pyrrole rings on protonation for **7**.

servation is consistent with the large chemical-shift difference for the DTT protons found in the ^{1}H NMR spectrum of **8**. The macrocyclic conjugation is nicely preserved because the pyrrole rings and DTT rings are in the same plane as that of the six *meso*-carbon atoms making dihedral angle almost zero in conformation with twisted double-sided Hückel topology.[20]

The octaphyrin **7**·2H$^+$ (with the TFA anion) crystallizes in the triclinic system with $P\bar{1}$ space group (Figure 3). The doubly twisted figure-eight conformation of the free-base was dramatically changed to an open conformation upon protonation. All the intramolecular hydrogen bonds ob-

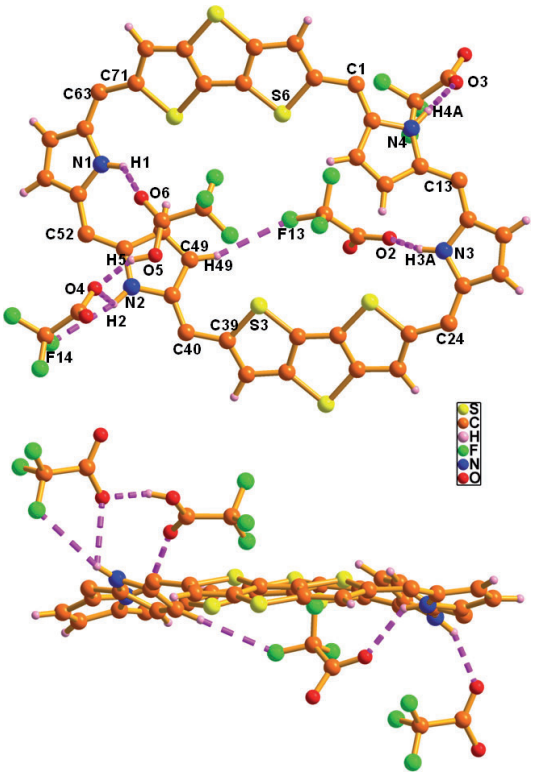

Figure 3. Single-crystal X-ray structure of **7**·2H$^+$. Top view (above) side view (below). For clarity, the *meso*-aryl groups are omitted in the top and side views.

served in the free-base are replaced by intermolecular hydrogen bonds with TFA counteranion. One pyrrole ring of each dipyrrin unit is inverted as reflected in the ^{1}H NMR spectroscopic analysis upon protonation. The distance between the two heterocyclic rings S6 and N3, and S3 and N1 are 7.28 and 7.36 Å, respectively, which is sufficient enough to accommodate two pyrrole β-CH protons inside the macrocyclic ring. There are four TFA molecules (O6, O4, O2, and O3), which are directly bound with the four pyrrolic NHs (N1-H1, N2-H2, N3-H3A, and N4-H4A) through intermolecular hydrogen-bonding interactions (N1-H1···O6; N2-H2···O4; N3-H3A···O2, and N4-H4A···O3) with distances of 2.33, 2.51, 2.21, and 2.10 Å, and angles of 135, 106, 140, and 152°, respectively. In addition, the N2 pyrrolic NH (N2-H2) and one of its β-CH protons (C49-H49) are in a intermolecular interaction with TFA fluorine atoms (F14 and F13) with the distance and angles of N2-H2···F14 and C49-H49···F13 are 2.85, 2.83 Å and 164, 162°, respectively. Out of the four TFA molecules, two TFA units are above and two are below the mean macrocyclic plane defined by six *meso*-carbons (C1, C13, C24, C40, C52, C63) with distances of 3.02, 2.21, 2.04, and 2.44 Å, respectively (Figure 3). On the other hand, the inverted pyrrolic units (N4, N2) are more deviated from the plane with respect to the normal (N3, N1) counterparts with the dihedral angles of 31.15, 24.16 and 13.28, 20.60°. However, the comparison of dihedral angles of *meso*-tolyl groups in free-base form (76 to 88°) and protonated derivative (50.34 to 39.7°) indicates a decrease in the protonated derivative suggesting the extension of conjugation. The observed torsion angles of 29.8 (C39-C40) and 24.3°(C63-C71) are within 30° and this allows π-electron conjugation in the extended structure of protonated derivative.[20,22]

Electronic absorption spectral studies: The electronic absorption spectra of **7** in CH_2Cl_2 shows broad and ill-defined peaks, with three major bands at 368, 524 and 724 nm without any distinct Q-bands (Figure 4). This is in contrast with

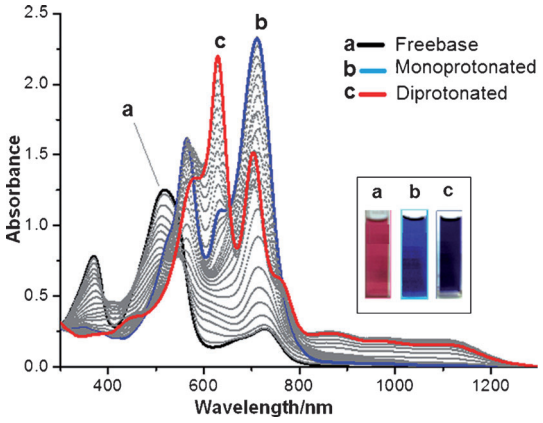

Figure 4. Titration of a dilute solution of TFA (0.1–100 mM) with **7** (0.01 mM) in CH_2Cl_2.

the absorption spectra of doubly fused rubyrin **6**, which exhibits an intense split Soret band in the region of 500–550 nm and weak Q-bands in the region of 600–900 nm (see the Supporting Information). Doubly fused rubyrins are known to be highly aromatic.[9b] Furthermore, the absorption spectra of **7** remain unaltered upon changing the polarity of the solvent (see the Supporting Information). Taken together, these observations suggest a nonaromatic nature of **7** and that the conformation of **7** remains intact upon changing the solvent polarity. The absorption spectra of **7** upon stepwise protonation using a dilute solution of TFA reveals definite spectral changes (Figure 4). Interestingly, broad absorption bands change to intense sharp ones with an increase in molar absorption coefficient accompanied by significant red-

shifts. Specifically, monoprotonated **7** shows a Soret-like band appearing at 568 and 696 nm with additional bands at 816 and 1136 nm. Further protonation leads to diprotonation resulting in a further shift of the bands to 416, 632, 701, and 992 nm. These observations reveal that a major structural change has taken place upon protonation.

The first look at changes in the absorption characteristics suggests that upon protonation, octaphyrins **7** and **8** might be aromatic in nature.[7b] However, theoretical calculations and the MO diagram does not support the presence of aromaticity in the diprotonated form (see below).

We have performed time-dependent (TD)-DFT calculations on the doubly fused rubyrin **6**, which is known to be aromatic. Keeping this as the reference, calculations were performed on both free-base and diprotonated forms of **7** and **8**. For **6**, from the MO diagram (see the Supporting Information), we confirmed the aromatic porphyrin-like features following typical Gouterman's four-orbital model.[23] These calculations revealed nearly degenerate HOMO/HOMO−1 and LUMO/LUMO−1 for **6**, which are characteristic of aromatic expanded porphyrins. A calculation of oscillator strength for the major transition of **6** reveals 96.58% for the transition from HOMO−1 to LUMO. On the other hand, the MO energy-level diagram of **7** shows a broken degeneracy for HOMO/HOMO−1, LUMO/LUMO+1 orbitals (Figure 5). The oscillator strength for the major transition is only 14% from HOMO−1 to LUMO+1 confirming the nonaromatic nature of the doubly fused octaphyrins in the free-base form.

The MO diagram calculated for the diprotonated derivative **7**·2H$^+$ reveals: 1) the perturbed degeneracy of HOMO/HOMO−1 and LUMO/LUMO+1; 2) a relatively small HOMO–LUMO gap, and 3) the same number of nodes for the frontier orbitals. These observations clearly suggest the antiaromatic nature of macrocycle in the diprotonated state (Figure 6).

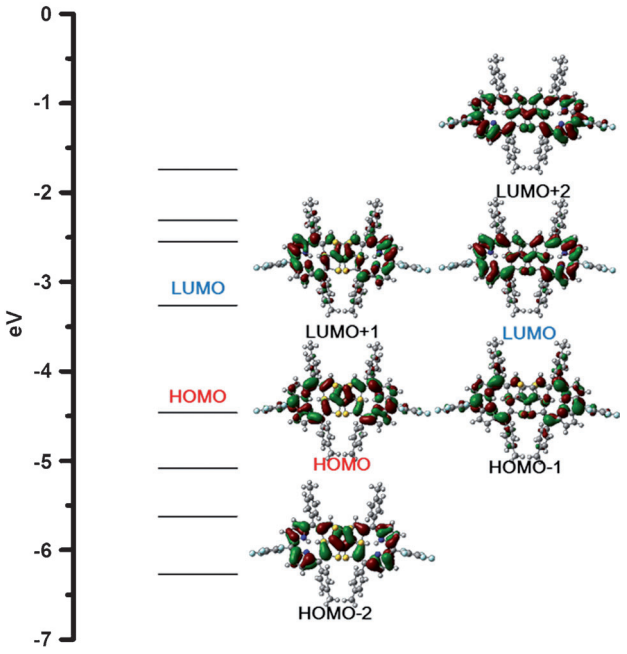

Figure 5. Molecular orbital diagram of **7**.

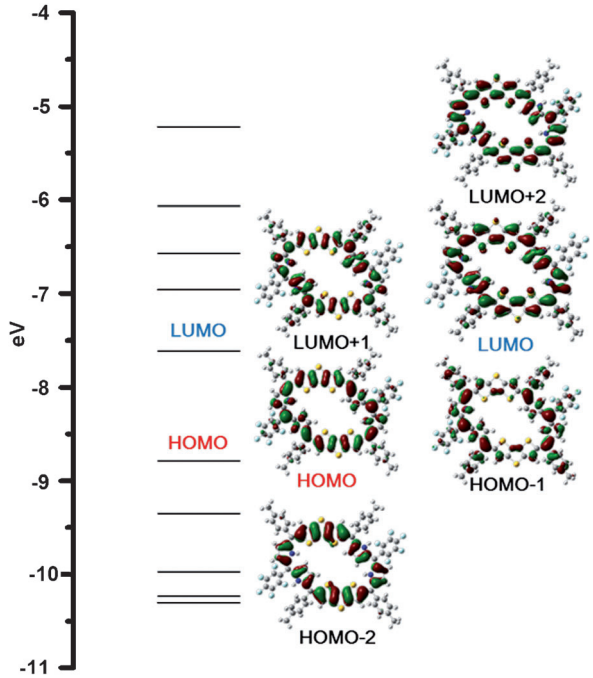

Figure 6. Calculated MO energy diagram of **7**·2H$^+$.

Theoretical calculations: We have calculated the optimized structures (B3LYP/6-311G(d,p))[24] for neutral and diprotonated octaphyrins by using the coordinates obtained from crystal structures of **8** and **7**·2H$^+$. Compared with the highly distorted conformation of the neutral form, the diprotonated octaphyrin reveals quite planar structures with distortions of pyrrole rings. Based on both the X-ray crystal and optimized structures, we have estimated the harmonic oscillator model of aromaticity (HOMA) and the bond-length alternation (BLA) values (Table 1).[25] Whereas the HOMA value increases, the BLA value decreases upon protonation. These features indicate that not only conformational changes but also an extension of π-conjugation is achieved upon protonation.

Table 1. HOMA and BLA values.

Structure		HOMA	BLA
neutral	X-ray	0.454	0.150
neutral	optimized	0.570	0.068
protonated	X-ray	0.557	0.133
protonated	optimized	0.587	0.058

To verify aromatic/antiaromatic characteristics in the extended protonated octaphyrins, we have adopted the nucleus-independent chemical shift (NICS)[26] and anisotropy-induced current density (AICD)[27] methods that are known

to be a good index for the aromaticity. Large positive NICS values were calculated at various geometrical positions (see the Supporting Information) of the diprotonated form (e.g., NICS(0) = 9.94 and NICS(1) = 9.34). And the NICS values at the central positions of pyrrole ($\delta = -1.54$ to $\approx +1.40$ ppm) and thiophene rings of DTT ($\delta = -12.60$ ppm) indicate its main conjugation pathway of 36π-electronic system. In addition, we have also attempted the direct visualization of the induced ring-current by using the AICD method, which describes the 3D image of delocalized electron densities with a scalar field. Since the AICD method illustrates the paramagnetic term of the induced current density, the aromatic molecules show clockwise current density and the antiaromatic species show counter-clockwise current density.

The AICD plot of diprotonated octaphyrin (see the Supporting Information) reveals clear counter-clockwise current-density vectors, thus indicating a paramagnetic ring-current. These results demonstrate that protonated octaphyrin has a Hückel antiaromatic character with continuous and paramagnetic current-density in its extended conformation.

Excited-state dynamics and optical nonlinear properties: We have investigated the excited-state dynamics of the neutral and protonated forms of octaphyrins by utilizing femtosecond transient absorption measurements (Figure 7). The transient species of neutral and protonated octaphyrins exhibit prominent excited-state absorption (ESA) and ground-state bleaching (GSB) signals corresponding to their steady-state absorption features[28] (Figure 4). The highly distorted neutral octaphyrin shows broad GSB and ESA signals in the entire spectral region. And the excited-state lifetime is estimated to be 0.6 (83%) and 8.8 ps (17%). We can assign the decay-time component of shorter than 1 ps as an energy relaxation processes from highest to lowest excited state such as a relaxation process from the S_2 to S_1 state.[29,30] However, despite spectral changes upon protonation, the transient species of protonated octaphyrins exhibit a reasonably fast excited-state lifetime. Also the small increase in lifetime observed for protonated derivatives reveals the rigidity of the macrocycle arising from the intermolecular hydrogen bonding interactions.[20,29]

We have also measured the TPA cross-section (σ^2) values for **7** and its protonated derivative by using a femtosecond Z-scan technique (Figure 8). The normal figure-eight octaphyrin **5** without any fused rings shows a TPA value of 870 GM.[16b] Compared with this, octaphyrin **7** reveals an increased TPA cross-section value of 1600 GM upon excitation at 1400 nm exhibiting the rigid fused moieties. Furthermore, upon protonation, the TPA cross-section values increased to 3200 and 2700 GM for mono and diprotonated forms, respectively. The TPA values in expanded porphyrin systems are known to depend on planarity, aromaticity, and the number of π-electrons in conjugation.[1,29] We and others have recently shown that an increase in aromaticity of the macrocycle results in a significant increase in the TPA values.[1] TPA values are also known to increase upon changing the topology from Hückel antiaromatic to the Möbius aromatic one.[14,20] The moderate increase in TPA values upon protonation in doubly fused octaphyrin is attributed to the structural change from figure-eight to an open-extended conjugated structure. The planarity of the DTT rings in the extended structure allows an extension of the π-conjugation. Changes in the polarization of π-electrons upon interaction with intense laser light are effective in the extended structure relative to the twisted figure-eight conformation leading to a moderate increase in the TPA values.[1]

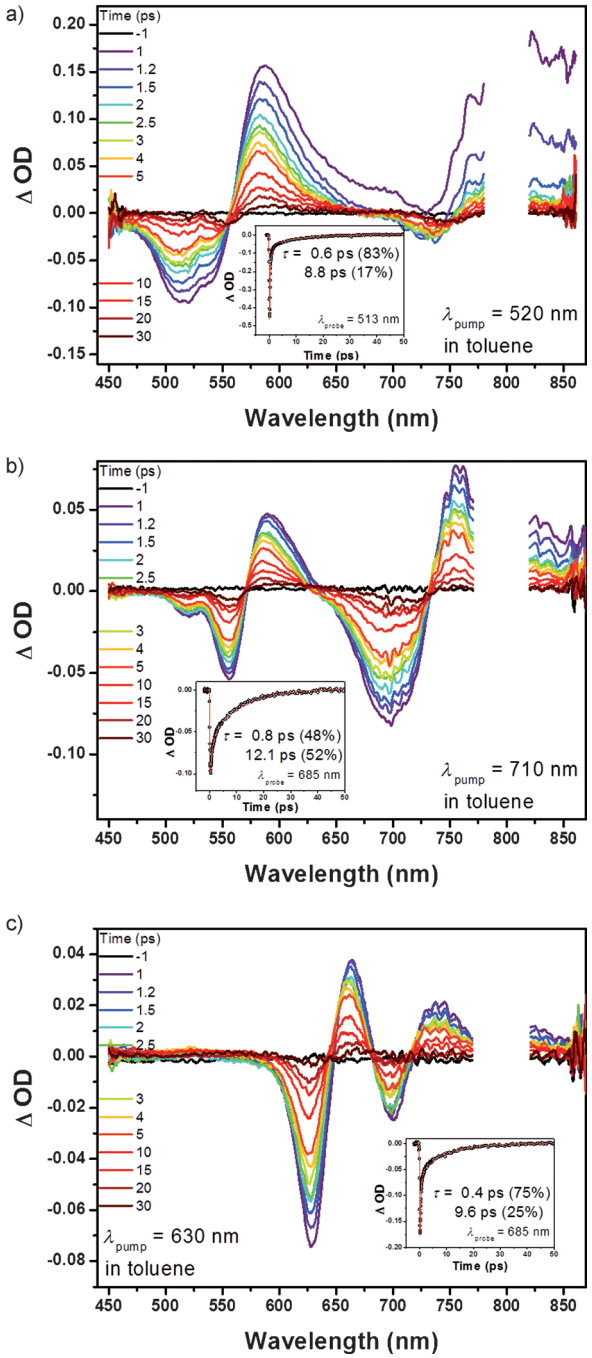

Figure 7. Femtosecond transient absorption spectra and representative decay profiles of a) **7**, b) **7**·H^+, and c) **7**·$2H^+$ in toluene.

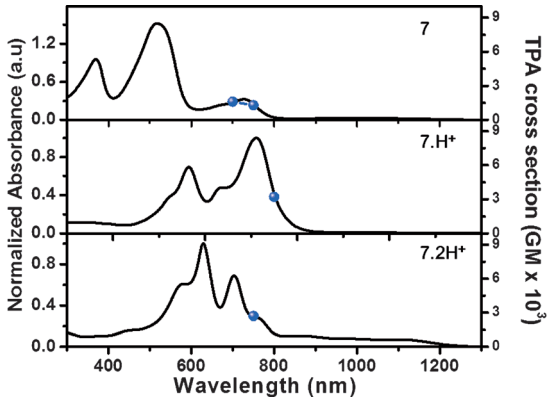

Figure 8. Steady-state absorption spectra (black line) and TPA cross-sections (spheres) of **7** (top), **7**·H$^+$ (middle), and **7**·2H$^+$ (bottom).

Conclusion

We have successfully synthesized and characterized two doubly fused 36π octaphyrins with the objective of designing a system that can switch over from an antiaromatic Hückel [4n]π topology to an aromatic [4n]π Möbius topology by an external chemical stimulation. The reasons for introducing fusion using rigid DTT rings, which are linked to each other through flexible dipyrrin subunits in the same macrocyclic framework, is to allow such a topology change. Even though we succeeded in achieving the expected topology change upon protonation, the switch over to Möbius aromaticity was not observed in the fused 36π octaphyrins. To attain Möbius aromatic stabilization in [4n]π systems, an appropriate mix between planarity and distortion within a macrocyclic framework is necessary so that the p orbitals containing the π-system would contain an odd number of nodes.[31] Obviously, in the fused 36π octaphyrins this is not achieved. Nevertheless, this study clearly demonstrates that change in the structure from a twisted figure-eight to an extended-open structure does not necessarily accompany the change to Möbius aromaticity in [4n]π systems.[14,20] We believe that the breaking of two intramolecular hydrogen bonding networks (N−H···N) in the free-base form and reformation of the six intermolecular hydrogen bonding networks (N−H···O, N−H···F, C−H···F) with the counteranion, is the driving force for such a structural change upon protonation.

The excited-state dynamics also give some insights into structural change upon protonation. Flexible figure-eight conformation of the free-base form is responsible for short singlet excited-state lifetimes since the flexibility provides an effective nonradiative decay pathway.[1c,29] However, in the diprotonated state, the presence of a rigid framework due to intermolecular hydrogen bonding and the presence of rigid DTT moiety partially destroys the effective nonradiative decay pathway and is responsible for the small increase in the singlet excited-state lifetime.[1c,29] The moderate increase in the TPA cross-section value upon protonation suggests that the perturbation of π electrons by femtosecond laser light is more effective in an extended structure relative to the twisted figure-eight structure.[1c,14,20] Further studies are in progress on a variety of expanded porphyrin systems to understand the structure–function correlation in this laboratory.

Experimental Section

Representative procedure for synthesis of DTT-dipyrrane: Pyrrole (3.66 mL) was added to 5,5′-bis-(mesitylhydroxylmethyl)dithienothiophene (DTT-mes-diol; 0.5 g) and the mixture was degassed by bubbling nitrogen gas. TFA (0.03 mL) was added to this solution and the reaction mixture was stirred for about 30 min at room temperature. After completion of the reaction, dichloromethane (100 mL) was added and the reaction mixture was neutralized with 0.1 M NaOH solution. The organic layer was separated and washed twice with water (50 mL) then dried over sodium sulfate. The solvent and excess pyrrole was removed by vacuum. The obtained product was purified by column chromatography over silica gel (100–200 mesh) with ethyl acetate/hexane (8:92, v/v). DTT-dipyrrane was obtained as yellow semi-solid.Yield:85%.

Compound **11**: ^{1}H NMR (400 MHz, $CDCl_3$, 298 K, TMS): $\delta = 7.89$ (br, 2H), 7.01 (s, 2H), 7.00 (d, 4H), 6.86 (d, 4H), 6.13 (m, 6H) 2.28 ppm (s, 6H); ESI-MS: *m/z* calcd for $C_{32}H_{26}N_2S_3+H^+$: 534.1258; found: 534.1378.

Compound **12**: ^{1}H NMR (400 MHz, $CDCl_3$, 298 K): $\delta = 8.24$ (br, 2H), 7.05 (s, 2H), 6.78 (s, 4H), 6.73 (s, 2H), 6.25 (m, 6H), 2.29 (s, 12H), 2.15 ppm (s, 6H); ESI-MS: *m/z* calcd for $C_{36}H_{34}N_2S_3+H^+$: 590.1884; found: 590.1127.

Representative procedure for the synthesis of doubly fused octaphyrins: Dry dichloromethane (200 mL) was added to DTT-dipyrrane (0.250 g, 0.42 mmol) and the mixture was degassed by bubbling nitrogen gas. Pentafluorobenzaldehyde (0.052 mL, 1 equiv) was added to this solution, and the reaction mixture was stirred for about 15 min at 298 K. Then 0.024 g (0.3 equiv) of *p*-TSA was added and stirring was continued for 2 h. DDQ (0.144 g, 1.5 equiv) was added to the reaction mixture and stirring was continued for further 2 h. The crude product obtained was purified by column chromatography over basic alumina followed by silica gel (100–200 mesh) with CH_2Cl_2/hexane (20:80, v/v). The pink color fraction was identified as product, after evaporation by vacuum yielded (7–10%) green-colored solid.

Compound **7**: ^{1}H NMR (400 MHz, $CDCl_3$, 298 K, TMS): $\delta = 15.48$ (brs, 2H), 9.38 (s, 2H), 6.85 (s, 2H), 7.41 (d, 8H), 7.25 (d, 8H), 6.32 (d, 2H), 6.30 (d, 2H), 5.87 (m, 4H), 2.48 (s, 6H), 2.45 ppm (s, 6H); **7**·2H$^+$: ^{1}H NMR (400 MHz, TFA/$CDCl_3$, 298 K, TMS): $\delta = 18.69$ (brs, 2H), 15.98 (d, 2H), 15.84 (d, 2H), 6.77 (d, 4H), 6.60 (d, 4H), 6.29 (d, 4H), 5.98 (d, 4H), 4.59 (d, 2H), 4.13 (d, 2H), 4.17 (s, 2H), 4.08 (s, 2H), 2.09 (s, 6H), 2.0 ppm (s, 6H); **7**: UV/Vis (CH_2Cl_2): λ_{max} (ε) = 368 (24300), 524 (33100), 608 (22200) 724 nm (10100 mol^{-1}m^{3}cm^{-1}); **7**·H$^+$ (TFA/CH_2Cl_2): λ_{max} (ε) = 452 (14900), 568 (48100), 696 (63500), 816 (7840), 1136 (2500), 1232 nm (2750 mol^{-1}m^{3}cm^{-1}); **7**·2H$^+$ (TFA/CH_2Cl_2): λ_{max} (ε) = 416 (10300), 632 (109000), 701 (93900), 992 nm (1300 mol^{-1}m^{3}cm^{-1}); **7**: ESI-MS: *m/z* calcd for $C_{78}H_{42}F_{10}N_4S_6+H^+$: 1417.1652; found: 1417.1589; elemental analysis calcd (%) for $C_{78}H_{42}F_{10}N_4S_6$: C 66.09, H 2.99, N 3.95; found: C 65.97, H 2.96, N 3.93.

Compound **8**: ^{1}H NMR (400 MHz, $CDCl_3$, 298 K, TMS): $\delta = 16.24$ (brs, 2H), 9.69 (s, 2H), 6.606 (s, 2H), 7.34 (s, 2H), 7.14 (s, 2H), 6.93 (s, 2H), 6.81 (s, 2H), 6.17 (d, 2H), 6.00 (d, 2H), 5.81 (m, 4H), 3.68 (s, 6H), 3.03 (s, 6H), 2.54 (s, 6H), 2.38 (s, 6H), 1.71 (s, 6H), 1.53 ppm (s, 6H); **8**·2H$^+$: ^{1}H NMR (400 MHz, TFA/$CDCl_3$, 298 K, TMS): $\delta = 23.03$ (brs, 2H), 17.84 (d, 2H), 17.67 (d, 2H), 6.38 (s, 4H), 6.25 (s, 4H), 3.79 (d, 2H), 3.55 (d, 2H), 3.09 (s, 2H), 2.90 (s, 2H), 2.07 (s, 12H), 1.96 (s, 12H), 1.90 (s, 6H), 1.81 ppm (s, 6H); **8**: UV/Vis (CH_2Cl_2): λ_{max} (ε) = 348 (70800), 528 (151300), 680 nm (27600 mol^{-1}m^{3}cm^{-1}); **8**·H$^+$ (TFA/CH_2Cl_2): λ_{max} (ε) = 392 (74400), 688 (295300), 816 (48800), 1188 (29100), 1176 nm (30600 mol^{-1}m^{3}cm^{-1}); **8**·2H$^+$ (TFA/CH_2Cl_2): λ_{max} (ε) = 388 (33800), 640 (196300), 688 (290800), 816 (17700), 1152 nm (13680 mol^{-1}m^{3}cm^{-1}); **8**: ESI-MS: *m/z*: calcd for $C_{86}H_{58}F_{10}N_4S_6+H^+$: 1529.2904; found: 1529.287;

elemental analysis calcd (%) for $C_{86}H_{58}F_{10}N_4S_6$: C 67.52, H 3.82, N 3.66; found: C 67.48, H 3.81, N 3.68.

^{1}H NMR measurements: ^{1}H NMR spectra were recorded on a Bruker (400 MHz) spectrometer. The NMR titration experiments were carried out with TFA solution dissolved in deutrated solvent. Variable-temperature measurements were performed for compound **7** in the [D_8]THF solvent.

Steady-state absorption measurement: Steady-state absorption spectra were obtained by using an UV/VIS/NIR spectrometer (Varian, Cary5000).

Femtosecond transient absorption measurement: The femtosecond time-resolved transient absorption (TA) spectrometer consisted of a home-made noncollinear optical parametric amplifier (NOPA) pumped by a Ti:-sapphire regenerative amplifier system (Quantronix, Integra-C) operating at 1 kHz repetition rate and an optical detection system. The generated visible NOPA pulses had a pulse width of approximately 100 fs and an average power of 1 mW in the range 500–700 nm, which were used as pump pulses. White-light continuum (WLC) probe pulses were generated using a sapphire window (3 mm of thickness) by focusing of small portion of the fundamental 800 nm pulses, which was picked off by a quartz plate before entering to the NOPA. The time delay between the pump and probe beams was controlled by making the pump beam travel along a variable optical delay (Newport, ILS250). Intensities of the spectrally dispersed WLC probe pulses are monitored by miniature spectrograph (OceanOptics, USB2000+). The polarization angle between the pump and probe beam was set at the magic angle (54.7°) to prevent polarization-dependent signals. The cross-correlation full-width at half-maximum (fwhm) in pump-probe experiments was less than 200 fs and chirp of WLC probe pulses was measured to be 800 fs in the 400–800 nm region. To minimize chirp, all reflection optics in probe beam path and 2 mm path length of quartz cell were used.

Two-photon absorption measurement: The TPA measurements were performed by using the open-aperture Z-scan method with 130 fs pulses from an optical parametric amplifier (Light Conversion, TOPAS) operating at a 2 kHz repetition rate using a Ti:sapphire regenerative amplifier system (Spectra-Physics, Hurricane X). After passing through an $f=$ 10 cm lens, the laser beam was focused to 1 mm-quartz cell. As the position of the sample cell was varied along the laser-beam direction (z-axis), the transmitted laser beam from the sample cell was then probed by using a Ge/PN photodiode (New Focus, 2033) as used for reference monitoring.

Quantum mechanical calculations: All calculations were carried out using the Gaussian 09 program. Initial geometries were obtained from X-ray structures. All structures were fully optimized without any symmetry restriction. The calculations were performed by the density functional theory (DFT) method with restricted B3LYP (Becke's three-parameter hybrid exchange functionals and the Lee–Yang–Parr correlation functional) level, employing a basis set 6–311G(d,p). The NICS values were obtained with the GIAO method at the B3LYP/6–311G(d,p) level. The global ring centers for the NICS values were designated at the non-weighted means of the carbon and sulfur coordinates on the peripheral positions of macrocycles. In addition, NICS values were also calculated on centers of other local cyclic structures as depicted in figures in the Supporting Information.

X-ray diffraction analysis: X-ray data were recorded on a BRUKER-APEX X-ray diffractometer equipped with a large area CCD detector. The structures were solved by Patterson synthesis and refined with the SHELX-97 programs. Single crystals of free-base **8** were obtained from vapor diffusion of acetonitrile into $CHCl_3$, whereas single crystals of **7**·2H$^+$ were obtained from vapor diffusion of acetonitrile into toluene. CCDC-930580 (**8**) and CCDC-930581 (**7**·2H$^+$) contain the supplementary crystallographic data for this paper. These data can be obtained free of charge from The Cambridge Crystallographic Data Centre via www.ccdc.cam.ac.uk/data_request/cif.

Acknowledgements

T.K.C. thanks the Department of Science and Technology (DST), New Delhi, India for the J. C. Bose Fellowship. We thank Dr. Arindam Ghosh and Dr. V. Krishnan for useful discussions on NMR spectroscopy and X-ray structures, respectively. The work at Yonsei University was supported by the World Class University Program (R32-10217) and Midcareer Researcher Program (2010-0029668) funded by the Ministry of Education, Science and Technology through the National Research Foundation of Korea.

[1] a) M. O. Senge, M. Fazekas, E. G. A. Notaras, W. J. Blau, M. Zawadzka, O. B. Locos, M. N. Mhuircheartaigh, *Adv. Mater.* **2007**, *19*, 2737–2774; b) J. Y. Shin, K. S. Kim, M. C. Yoon, J. M. Lim, Z. S. Yoon, A. Osuka, D. Kim, *Chem. Soc. Rev.* **2010**, *39*, 2751–2767; c) J. M. Lim, Z. S. Yoon, J. Y. Shin, K. S. Kim, M. C. Yoon, D. Kim, *Chem. Commun.* **2009**, 261–273; d) T. K. Chandrashekar, S. Venkataraman, *Acc. Chem. Res.* **2003**, *36*, 676–696; e) R. Misra, R. Kumar, T. K. Chandrashekar, C. H. Suresh, A. Nag, D. Goswami, *J. Am. Chem. Soc.* **2006**, *128*, 16083–16091; f) H. Rath, J. Sankar, V. Prabhuraja, T. K. Chandrashekar, A. Nag, D. Goswami, *J. Am. Chem. Soc.* **2005**, *127*, 11608–11609.

[2] a) R. Bonnett, *Chem. Soc. Rev.* **1995**, *24*, 19–33; b) J. L. Sessler, S. J. Weghorn, *Expanded, Contracted and Isomeric Porphyrins*, Pergamon, New York, **1997**, *15*, 429–503; c) C. R. Karunakaran, P. S. S. Babu, M. B. Betsy, K. P. Albish, A. S. Nair, K. S. Rao, A. Srinivasan, T. K. Chandrashekar, C. M. Rao, R. Pillai, D. Ramaiah, *ACS Chem. Biol.* **2013**, *8*, 127–132.

[3] a) A. Jasat, D. Dolphin, *Chem. Rev.* **1997**, *97*, 2267–2340; b) A. Srinivasan, M. V. R. Reddy, S. J. Narayanan, B. Sridevi, K. S. Pushpan, M. Ravikumar, T. K. Chandrashekar, *Angew. Chem.* **1997**, *109*, 2710–2713; *Angew. Chem. Int. Ed. Engl.* **1997**, *36*, 2598–2601; c) B. Sridevi, S. J. Narayanan, R. Rao, T. K. Chandrashekar, U. Englich, K. R. Senge, *Inorg. Chem.* **2000**, *39*, 3669–3677.

[4] M. B. Winter, P. J. Klemm, C. M. Phillips-Piro, K. N. Raymond, M. A. Marletta, *Inorg. Chem.* **2013**, *52*, 2277–2279.

[5] a) Z. S. Yoon, A. Osuka, D. Kim, *Nat. Chem.* **2009**, *1*, 113–122; b) J. Wu, I. Fernandez, P. v. R. Schleyer, *J. Am. Chem. Soc.* **2013**, *135*, 315–321.

[6] a) R. Misra, T. K. Chandrashekar, *Acc. Chem. Res.* **2008**, *41*, 265–279; b) Y. Pareek, M. Ravikanth, T. K. Chandrashekar, *Acc. Chem. Res.* **2012**, *45*, 1801–1816.

[7] a) M. Stępień, N. Sprutta, L. Latos-Grażyński, *Angew. Chem.* **2011**, *123*, 4376–4430; *Angew. Chem. Int. Ed.* **2011**, *50*, 4288–4340; b) S. Saito, A. Osuka, *Angew. Chem.* **2011**, *123*, 4432–4464; *Angew. Chem. Int. Ed.* **2011**, *50*, 4342–4373.

[8] a) P. J. Chmielewski, L. Latos-Grażyński, K. Rachlewicz, *Chem. Eur. J.* **1995**, *1*, 68–72; b) N. Sprutta, L. Latos-Grażyński, *Org. Lett.* **2001**, *3*, 1933–1935; c) S. Shimizu, R. Taniguchi, A. Osuka, *Angew. Chem.* **2005**, *117*, 2265–2269; *Angew. Chem. Int. Ed.* **2005**, *44*, 2225–2229.

[9] a) H. Furuta, T. Ishizuka, A. Osuka, T. Ogawa, *J. Am. Chem. Soc.* **1999**, *121*, 2945–2946; b) T. K. Chandrashekar, V. Prabhuraja, S. Gokulnath, R. Sabarinathan, A. Srinivasan, *Chem. Commun.* **2010**, *46*, 5915–5917.

[10] a) H. Furuta, T. Asano, T. Ogawa, *J. Am. Chem. Soc.* **1994**, *116*, 767–768; b) P. J. Chmielewski, L. Latos-Grażyński, K. Rachlewicz, T. Glowiak, *Angew. Chem.* **1994**, *106*, 805–808; *Angew. Chem. Int. Ed. Engl.* **1994**, *33*, 779–781.

[11] E. Vogel, M. Bröring, J. Fink, D. Rosen, H. Schmickler, J. Lex, K. W. K. Chan, Y.-D. Wu, D. A. Plattner, M. Nendel, K. N. Houk, *Angew. Chem.* **1995**, *107*, 2705–2709; *Angew. Chem. Int. Ed. Engl.* **1995**, *34*, 2511–2514.

[12] a) A. Osuka, S. Saito, *Chem. Commun.* **2011**, *47*, 4330–4339; b) E. Pacholska-Dudziak, J. Skonieczny, M. Pawlicki, L. Szterenberg, Z. Ciunik, L. Latos-Grażyński, *J. Am. Chem. Soc.* **2008**, *130*, 6182–6195.

[13] a) G. Karthik, M. Sneha, V. Prabhuraja, J. M. Lim, D. Kim, A. Srinivasan, T. K. Chandrashekar, *Chem. Eur. J.* **2013**, *19*, 1886–1890;

b) V. G. Anand, S. Saito, S. Shimizu, A. Osuka, *Angew. Chem.* **2005**, *117*, 7410–7414; *Angew. Chem. Int. Ed.* **2005**, *44*, 7244–7248; c) M. Suzuki, A. Osuka, *J. Am. Chem. Soc.* **2007**, *129*, 464–465.

[14] S. Saito, J. Y. Shin, J. M. Lim, K. S. Kim, D. Kim, A. Osuka, *Angew. Chem.* **2008**, *120*, 9803–9806; *Angew. Chem. Int. Ed.* **2008**, *47*, 9657–9660.

[15] M. Alonso, P. Geerlings, F. D. Proft, *Chem. Eur. J.* **2013**, *19*, 1617–1622.

[16] a) S. Mori, A. Osuka, *J. Am. Chem. Soc.* **2005**, *127*, 8030–8032; b) Y. Tanaka, S. Saito, S. Mori, N. Aratani, H. Shinokubo, N. Shibata, Y. Higuchi, Z. S. Yoon, K. S. Kim, S. B. Noh, J. K. Park, D. Kim, A. Osuka, *Angew. Chem.* **2008**, *120*, 693–696; *Angew. Chem. Int. Ed.* **2008**, *47*, 681–684.

[17] M. Stępień, L. Latos-Grażyński, N. Sprutta, P. Chwalisz, L. Szterenberg, *Angew. Chem.* **2007**, *119*, 8015–8019; *Angew. Chem. Int. Ed.* **2007**, *46*, 7869–7873.

[18] J. Sankar, S. Mori, S. Saito, H. Rath, M. Suzuki, Y. Inokuma, H. Shinokubo, K. S. Kim, Z. S. Yoon, J. Y. Shin, J. M. Lim, Y. Matsuzaki, O. Matsushita, A. Muranaka, N. Kobayashi, D. Kim, A. Osuka, *J. Am. Chem. Soc.* **2008**, *130*, 13568–13579.

[19] J. K. Park, Z. S. Yoon, M. C. Yoon, K. S. Kim, S. Mori, J. Y. Shin, A. Osuka, A. D. Kim, *J. Am. Chem. Soc.* **2008**, *130*, 1824–1825.

[20] J. M. Lim, J. Y. Shin, Y. Tanaka, S. Saito, A. Osuka, D. Kim, *J. Am. Chem. Soc.* **2010**, *132*, 3105–3114.

[21] a) O. K. Kim, K. S. Lee, H. Y. Woo, K. S. Kim, G. S. He, J. Swiatkiewicz, P. N. Prasad, *Chem. Mater.* **2000**, *12*, 284–290; b) J. Frey, A. D. Bond, A. B. Holmes, *Chem. Commun.* **2002**, 2424–2425; c) I. Palamà, F. D. Maria, I. Viola, E. Fabiano, G. Gigli, C. Bettini, G. Barbarella, *J. Am. Chem. Soc.* **2011**, *133*, 17777–17785.

[22] Z. Zhang, J. M. Lim, M. Ishida, V. Roznyatovskiy, V. Lynch, H. Y. Gong, X. Yang, D. Kim, J. L. Sessler, *J. Am. Chem. Soc.* **2012**, *134*, 4076–4079.

[23] M. Gouterman, *J. Mol. Spectrosc.* **1961**, *6*, 138–163.

[24] a) A. D. J. Becke, *J. Chem. Phys.* **1993**, *98*, 1372–1377; b) C. Lee, W. Yang, R. G. Parr, *Phys. Rev. B* **1988**, *37*, 785–790.

[25] T. M. Krygowski, *J. Chem. Inf. Comput. Sci.* **1993**, *33*, 70–78; b) T. M. Krygowski, M. K. Cyranski, *Chem. Rev.* **2001**, *101*, 1385–1390.

[26] a) J. Kruszewski, T. M. Krygowski, *Tetrahedron Lett.* **1972**, *13*, 3839–3842; b) P. v. R. Schleyer, C. Maerker, A. Dransfeld, H. Jiao, N. J. R. E. Hommes, *J. Am. Chem. Soc.* **1996**, *118*, 6317–6318.

[27] a) D. Geuenich, K. Hess, F. Kohler, R. Herges, *Chem. Rev.* **2005**, *105*, 3758–3772; b) E. Steiner, P. W. Fowler, *Org. Biomol. Chem.* **2006**, *4*, 2473–2476.

[28] R. Berera, R. v. Grondelle, J. T. M. Kennis, *Photosynth. Res.* **2009**, *101*, 105–118.

[29] M. C. Yoon, R. Misra, Z. S. Yoon, K. S. Kim, J. M. Lim, T. K. Chandrashekar, D. Kim, *J. Phys. Chem. B* **2008**, *112*, 6900–6909.

[30] J. Y. Shin, J. M. Lim, Z. S. Yoon, K. S. Kim, M. C. Yoon, S. Hiroto, H. Shinokubo, S. Shimizu, A. Osuka, D. Kim, *J. Phys. Chem. B* **2009**, *113*, 5794–5802.

[31] E. Heilbronner, *Tetrahedron Lett.* **1964**, *5*, 1923–1928.

Received: May 26, 2013
Published online: November 6, 2013

